World Academy of Science, Engineering and Technology
International Journal of Chemical and Materials Engineering
Vol:12, No:11, 2018

Formation of Protective Aluminum-Oxide Layer on the Surface of Fe-Cr-Al Sintered-Metal-Fibers via Multi-Stage Thermal Oxidation

Loai Ben Naji, Osama M. Ibrahim, Khaled J. Al-Fadhalah

***Abstract*—**The objective of this paper is to investigate the formation and adhesion of a protective aluminum-oxide (Al_2O_3, alumina) layer on the surface of Iron-Chromium-Aluminum Alloy (Fe-Cr-Al) sintered-metal-fibers. The oxide-scale layer was developed via multi-stage thermal oxidation at 930 ^oC for 1 hour, followed by 1 hour at 960 ^oC, and finally at 990 ^oC for 2 hours. Scanning Electron Microscope (SEM) images show that the multi-stage thermal oxidation resulted in the formation of predominantly Al_2O_3 platelets-like and whiskers. SEM images also reveal non-uniform oxide-scale growth on the surface of the fibers. Furthermore, peeling/spalling of the alumina protective layer occurred after minimum handling, which indicates weak adhesion forces between the protective layer and the base metal alloy. Energy Dispersive Spectroscopy (EDS) analysis of the heat-treated Fe-Cr-Al sintered-metal-fibers confirmed the high aluminum content on the surface of the protective layer, and the low aluminum content on the exposed base metal alloy surface. In conclusion, the failure of the oxide-scale protective layer exposes the base metal alloy to further oxidation, and the fragile non-uniform oxide-scale is not suitable as a support for catalysts.

***Keywords*—**High-temperature oxidation, alumina protective layer, iron-chromium-aluminum alloy, sintered-metal-fibers.

I. Introduction

ALLOYS containing aluminum, such as Fe-Cr-Al, are designed to form an Al_2O_3 layer to protect the base metal alloy surface from further oxidation at high temperatures. The oxide-scale layer is usually developed via single or multi-stage thermal oxidation. Fe-Cr-Al contains mainly iron, chromium, and aluminum. The relatively high concentrations of aluminum and chromium increase the thermal resistance at high temperature by forming a protective oxide-scale layer on the surface. In addition, a small fraction less than 0.5% of rare earth elements, such as yttrium, zirconium, and cerium, are commonly added to Fe-Cr-Al to enhance its oxidation characteristics at high temperature and improve the adhesion between the oxide-scale layer and the base metal alloy [1]-[3]. Strawbridge and Hou [4] investigated the effects of rare earth elements on the formation and adhesion of the oxide-scale layer. Their study cited that rare earth elements had a significant improvement in the oxide-scale adherence on aluminum-containing alloys during isothermal and cyclic oxidation. A similar study by Ishii et al. [5] investigated the effect of rare earth elements on high-temperature oxidation of metal foils made of Fe-Cr-Al. The study cited that the rare earth elements prevent oxygen grain boundary diffusion, and Al_2O_3 scale growth rate can be decreased with increasing rare earth elements content.

Thermal oxidation of Fe-Cr-Al can also lead to interesting Al_2O_3 morphology formations with high surface area such as platelets or whiskers [6]-[8]. Thermal oxidation temperature and exposure time affect the formation of Al_2O_3 phases on the metal surface, which depend on conditions such as thermal oxidation technique, impurities, and crystallinity that found on the alloy base-metal [9]. Fei et al. [10] reported that during thermal oxidation temperatures between 800 and 900 ^oC metastable alumina platelets and whiskers mainly arranged on the surface. They also reported that the rapid growth rate of the Al_2O_3 could deplete the aluminum content from the base metal alloy. Pint et al. [11] concluded that the transformation of the metastable, which consists mainly of θ-Al_2O_3, into stable α-Al_2O_3, causes volume change. This volume change could result in microcracks leading to failure of the protective oxide-scale layer. In a related note, Kadiri et al. [7] studied single-stage thermal oxidation at 900 ^oC for 5 hours on metal foils made of Fe-Cr-Al, which resulted in the formation of oxide nodules and crater on the surface. At the oxide crater nodule boundary, there was a radial arrangement of the platelets or whiskers. Kadiri et al. [7] reported that the changing in the oxide volume causes tensile stresses, which led to the formation of cracks and affected the adhesion of the oxide layer to the surface of the base metal alloy.

A technical paper by Samad et al. [8] presented results for multi-stage thermal oxidation of Fe-Cr-Al sintered-metal-fibers as a catalyst support. Their focus was to study the formation of α-Al_2O_3 whiskers as support for palladium-based catalyst. The thermal oxidation process started at a lower temperature and later continued with higher temperatures to accelerate the growth rate of the alumina layer on the surface of the fibers. Explicitly, the fibers were heated at three temperature steps: at 930 ^oC for 1 hour, 960 ^oC for 1 hour and finally at 990 ^oC for 2 hours. Their results show that the surface of the oxide-scale is predominantly covered with α-Al_2O_3 whiskers of 203±34 nm in height and 100–200 nm apart; where θ-Al_2O_3 phase has also existed on the surface of the fibers. Furthermore, the multi-stage thermal oxidation was

Mr. Ben Naji is an instructor at the Mechanical Power Department, The Higher Institute of Energy, Kuwait (e-mail: lm.binnaji@paaet.edu.kw).

Dr. Ibrahim was a CTO at Rypos, Inc., Franklin, MA 02038 USA. He is now an Associate Professor at the Mechanical Engineering Department, Kuwait University (e-mail: Osama.ibrahim@ku.edu.kw).

Dr. Al-Fadhalah is an Associate Professor the Mechanical Engineering Department, Kuwait University (e-mail: khaled.alfadhalah@ku.edu.kw).

found to decrease the total time necessary for the growth of the oxide layer compared with isothermal oxidation [12]. However, the rapid growth rate of Al_2O_3 on the alloy surface is likely to reduce the limited aluminum content in the base metal alloy, which could restrict the lifetime of the Fe-Cr-Al fibers [11], [13], [14].

In the current study, the objective is to investigate the formation and adhesion of the aluminum oxide layer on the surface of Fe-Cr-Al sintered-metal-fibers. SEM high-resolution images and EDS analysis were performed on two samples. The first sample was kept without heat treatment as a baseline, while the second sample was heat treated using multi-stage thermal oxidation.

II. Sample Preparation

Two sintered-metal-fibers samples were cut to 1 cm in diameter and cleaned with methanol in an ultrasonic bath for 30 minutes. The samples then were dried in an oven at 120 ºC for 1 hour. The first sample, Sample 1, was kept without heat treatment as a baseline, and the second sample, Sample 2, was heat treated via multi-stage thermal oxidation similar to Samad et al. [8] as shown in Table I. The chemical compositions of the tested Fe-Cr-Al fibers are shown in Table II.

TABLE I
Sample Preparation

Sample	Heat treatment temperature and time
1	No heat treatment
2	930 ºC for 1 hour 960 ºC for 1 hour 990 ºC for 2 hours

TABLE II
The Chemical Compositions of the Sintered-Metal-Fibers

Element	Chemical composition (%)
Cr	20.580
Al	5.760
Mn	0.160
Cu	0.046
Ti	0.041
C	0.033
P	0.015
S	0.002
N	0.010
Si	0.240
Fe	Balance

III. Test Procedure

EDS analysis was performed to obtain the elemental identification and composition on the surface of the fibers; while SEM was utilized to obtain detailed high-resolution images of the surface morphology.

IV. Results and Discussion

Two samples were investigated in this study. Sample 1, which was not heat treated, represents the baseline while Sample 2 was heat treated by the multi-stage thermal oxidation as described in the sample preparation section, Table I. Fig. 1 shows SEM micrographs of Sample 1 and the selected areas of Spectrum 1 and Spectrum 2. SEM micrographs also show non-uniform distributions of nodules all over the surface of Sample 1 fibers. The EDS analysis of Sample 1 shows that there is a variation in the elemental composition between Spectrum 1 and Spectrum 2. Spectrum 1 represents the micrograph of the flat area, while Spectrum 2 represents the spot scan area of nodules on the surface of the metal-fiber. Fig. 2 shows the results of the EDS analysis of Spectrum 1 and Spectrum 2. Compared to Spectrum 2, Spectrum 1 has slightly more iron content, and approximately the same chromium and oxygen contents, but less aluminum. The results show that the nodules have high aluminum content compared to the flat area, which has approximately similar elemental composition to the base metal alloy shown in Table II.

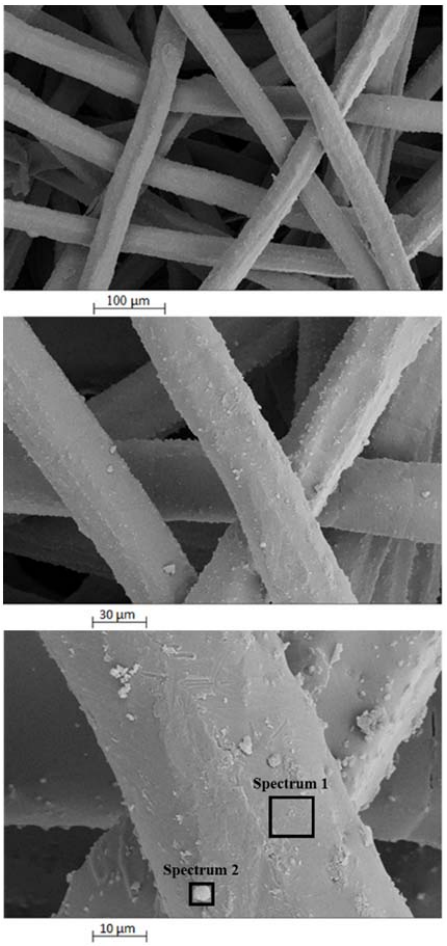

Fig. 1 Sintered-metal-fibers without heat treatment, Sample 1

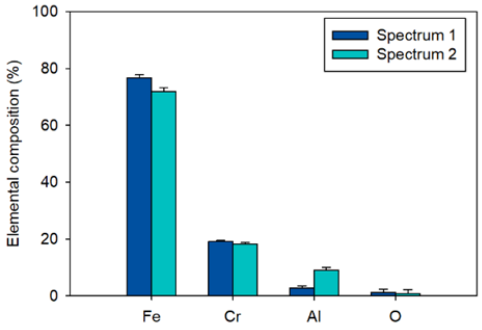

Fig. 2 Elemental composition of Sample 1; Spectrum 1 represents the micrograph of the flat area, and Spectrum 2 represents the spot scan area of nodules

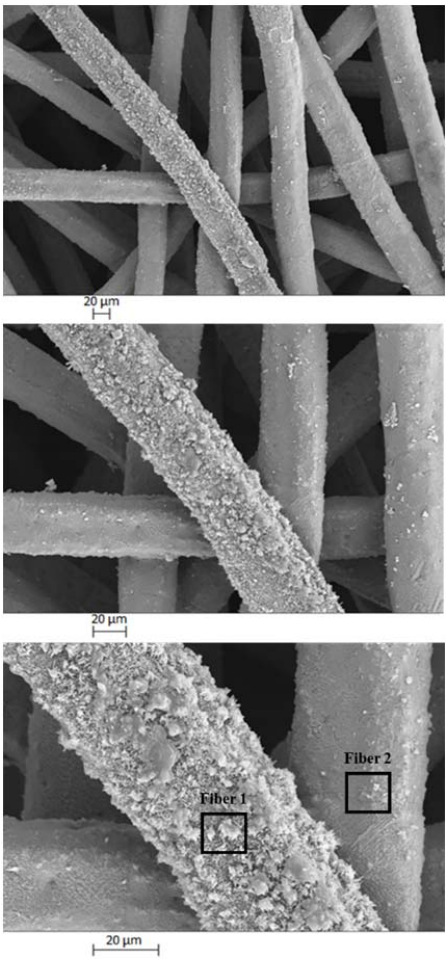

Fig. 3 Sample 2 heat treated via multi-stage oxidation

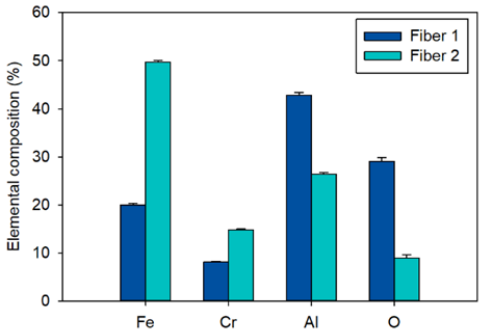

Fig. 4 Elemental composition of Fiber 1 and Fiber 2 of Sample 2; Fiber 1 shows a forest with platelets/whiskers morphology, while Fiber 2 shows relatively a smooth oxide-scale layer

Fig. 3 shows two adjacent fibers. Fiber 1 shows a forest with platelets-like and whiskers morphology, while Fiber 2 shows relatively a smooth oxide-scale layer with no distinct features on the fiber surface. Elemental composition of Fibers 1 and 2 of Sample 2 is displayed in Fig. 4. Compared to Fiber 2, the results show that the surface of Fiber 1 has more aluminum and oxygen, and less iron and chromium. The results indicate there is more aluminum diffusion resulting in aluminum oxide formation on Fiber 1 than Fiber 2. Furthermore, the elemental composition of Sample 2 shows high aluminum and oxygen on the surface compared to the baseline Sample 1, which confirms the formation of the Al_2O_3 protective layer on both fibers by the multi-stage thermal oxidation. SEM analysis also shows the peeling/spalling of the Al_2O_3 layer on the Fe-Cr-Al fibers after minimum handling of Sample 2, as shown in Fig. 5. This peeling condition indicates poor adhesion between the oxide-scale layer and the base metal alloy. Fig. 6 shows the comparison between elemental composition of the exposed surface, Spectrum 1, and the top of the spalled layer, Spectrum 2. The EDS results reveal that the exposed surface (Spectrum 1) appears to be smooth and showed a chemical composition similar to the baseline of Fe-Cr-Al alloy content shown in Table II. The results also show that Spectrum 2 has less iron and higher contents of aluminum and oxygen than Spectrum 1. The high aluminum content of Spectrum 2 is due to the dense growth of platelets-like or whiskers of the oxide-aluminum protective layer.

V. Conclusions

The current work investigated the formation of the Al_2O_3 protective layer on the surface of sintered-metal-fibers made of Fe-Cr-Al alloy. In this study, multi-stage heat treatment was considered. SEM-EDS analyses were performed to investigate the growth of the oxide-scale protective layer, formed on the fiber surface. Thermal oxidation of Fe-Cr-Al alloy microfibers resulted in the formation of predominantly Al_2O_3 platelets-like and whiskers. The SEM images further reveal that the oxide-scale layer was not uniform on the surface of the fibers. The SEM images also show the peeling/ spalling of the oxide-scale protective layer after minimum

handling, which indicates poor adhesion between the oxide-scale layer and the base metal alloy. It's known that the multi-stage thermal oxidation accelerates the growth rate of the Al_2O_3 protective layer [12]. The rapid growth rate and the phase transformation of the Al_2O_3 layer can cause internal stresses due to the variation in volume and thermal expansion leading to cracks and spalling of the protective oxide-scale layer. The chemical composition analysis of the tested samples, made of Fe-Cr-Al alloy, did not include the rare earth elements. Several studies showed that the rare earth elements are added to the Fe-Cr-Al metal alloy to reduce the oxide layer growth and improve the adhesion between the oxide-scale protective layer and the base metal alloy [1]-[5]. The failure of the oxide-scale protective layer exposes the base metal to further oxidation, and the fragile non-uniform oxide-scale is not suitable as a support for catalysts.

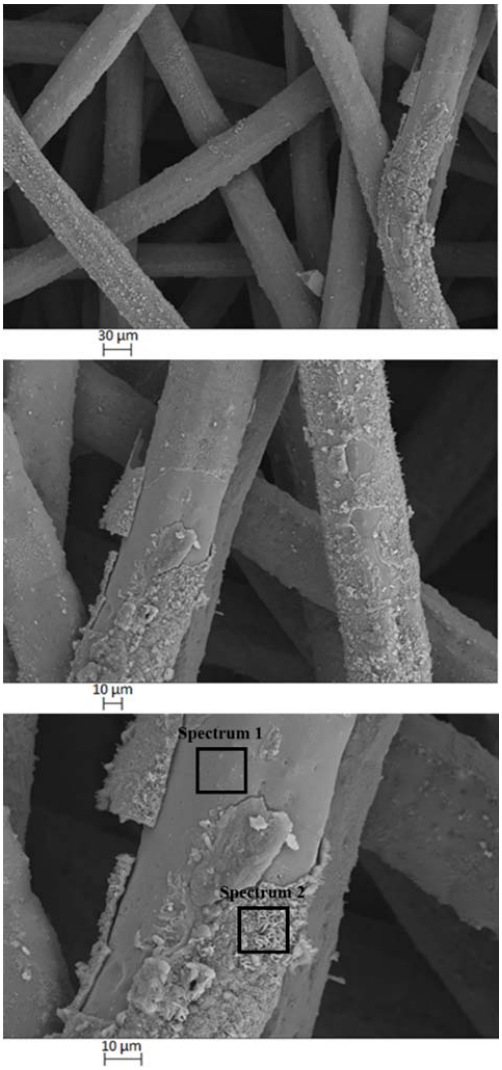

Fig. 5 Peeling/spalling of the protective layer of Sample 2

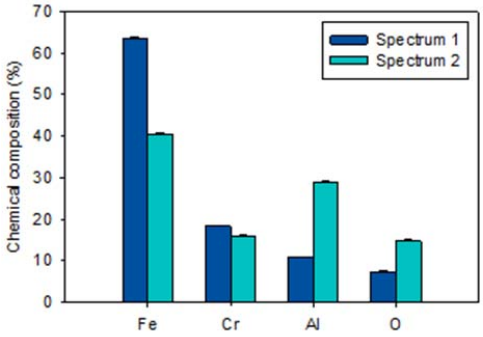

Fig. 6 Sample 2 after the peeling/spalling of the protective layer. Spectrum 1 represents the exposed surface under the protective oxide-scale layer, while Spectrum 2 represents the top of spalled oxide-scale layer

ACKNOWLEDGMENT

We gratefully acknowledge the support of Kuwait University under grant numbers RE04/16 and GE01/07. We also acknowledge the support of Kuwait Foundation for the Advancement of Science.

REFERENCES

[1] D. Whittle, and J. Stringer, "Dispersions resistance by additions of reactive elements or oxide improvements in high-temperature oxidation," *Philosophical Transactions of the Royal Society A*, 295, 1980, doi: 10.1098/rsta.1980.0124.

[2] R. Prescott, and M. Graham, "The formation of aluminum oxide scales on high-temperature alloys," *Oxidation of Metals*, Vol. 38, Nos. 3/4, 1992.

[3] J. Herbelin, and M. Mantel, "Effects of Al Addition and Minor Elements on Oxidation Behaviour of FeCr Alloys," *Journal de Physique IV Colloque*, 05 (C7), pp.C7-365-C7-374, 1995.

[4] A. Strawbridge and P. Hou, "The role of reactive elements in oxide scale adhesion," *Materials at High Temperatures*, 12:2-3, 177-181, 1994, doi: 10.1080/09603409.1994.11689484.

[5] K. Ishii, M. Kohno, S. Ishikawa, and S. Satoh, "Effect of rare-earth elements on high-oxidation resistance of Fe-20Cr-5Al alloy foils," *Materials Transactions*, JIM, Vol. 38, No. 9, pp 787-792, 1997.

[6] C. Badini, and F. Laurella, "Oxidation of FeCrAl alloy: influence of temperature and atmosphere on scale growth rate and mechanism," *Surface and Coatings Technology*, 135 291–298, 2001.

[7] H. Kadiri, H. Molins, Y. Bienvenu, and M. Horstemeyer, "Abnormal high growth rates of metastable aluminas on FeCrAl alloys, " Oxidation *of Metals*, 64: 63-97, 2005 doi: 10.1007/s11085-005-5715-0.

[8] J. Samad, J. Nychka, and N. Semagina, "Structured catalysts via multiple stage thermal oxidation synthesis of FeCrAlly alloy sintered microfibers," *Chemical Engineering Journal*, 168 470–476, 2011.

[9] R. Zhou, and R. Snyder, "Structures and transformation mechanisms of the Eta. Gamma and Theta transition aluminas," *Acta Crystallographica Section B*, 47 617–630, 1991.

[10] W. Fei, S. Kuiry, and S. Seal, "Inhibition of metastable alumina formation on Fe–Cr–Al–Y alloy fibers at high temperature using titania coating," *Oxidation of Metals*, 62 29–44, 2004.

[11] B. Pint, J. Martin, and L. Hobbs," The oxidation mechanism of θ-Al_2O_3 scales," *Solid State Ionics*, 78, 99-107, 1995.

[12] G. Vaneman, and D. Sigler, "Accelerated whisker growth on iron–chromium–aluminum alloy foil," Patent US 4915751, 1990.

[13] R. Molins, A. Germidis, and E. Andrieu, in Microscopy of Oxidation 3: Proceedings of the Third International Conference on the Microscopy of Oxidation. S. B. Newcomb and J. A. Little, eds., p. 3, Institute of Materials, London, 1997.

[14] C. Badini, and F. Laurella, "Oxidation of FeCrAl alloy: influence of temperature and atmosphere on scale growth rate and mechanism," *Surface and Coatings Technology,* 135, 291-298, 2001.